Structural Engineering and Mechanics, Vol. 9, No. 4 (2000) 323-338
DOI: http://dx.doi.org/10.12989/sem.2000.9.4.323

Nonlinear analysis and tests of steel-fiber concrete beams in torsion

Chris G. Karayannis†

Department of Civil Engineering, Democritus University of Thrace, Xanthi 67100, Greece

Abstract. An analytical approach for the prediction of the behaviour of steel-fiber reinforced concrete beams subjected to torsion is described. The analysis method employs a special stress-strain model with a non-linear post cracking branch for the material behaviour in tension. Predictions of this model for the behaviour of steel-fiber concrete in direct tension are also presented and compared with results from tests conducted for this reason. Further in this work, the validation of the proposed torsional analysis by providing comparisons between experimental curves and analytical predictions, is attempted. For this purpose a series of 10 steel-fiber concrete beams with various cross-sections and steel-fiber volume fractions tested in pure torsion, are reported here. Furthermore, experimental information compiled from works around the world are also used in an attempt to establish the validity of the described approach based on test results of a broad range of studies. From these comparisons it is demonstrated that the proposed analysis describes well the behaviour of steel-fiber concrete in pure torsion even in the case of elements with non-rectangular cross-sections.

Key words: steel-fiber concrete; torsion; nonlinear analysis; tensional model; torsional tests; L and T-beams.

1. Introduction

The analytical prediction of the behaviour of concrete elements in torsion is an open problem in the field of the design of concrete structures. It has been deduced by early experimental efforts that the response of an element in pure torsion is greatly influenced by the behaviour of the material in direct tension (Anderson 1935, Cowan 1965). Thus, in order to enhance the torsional behaviour of concrete elements, the improvement of the poor performance of concrete in tension by incorporating steel-fibers, has been proposed and extensively used in the last decades (ACI 1982, Lim *et al*. 1987, Gopalaratnam and Shah 1987, Bentur and Mindness 1990). Moreover, in this case the phenomenon of torsion of steel-fiber concrete elements has been even more open to question and although considerable theoretical and experimental research has been carried out on the behaviour of steel-fiber concrete in direct tension, bending and shear, comparatively little attention has been paid to its behaviour in torsion.

The elastic response of homogeneous structural elements in torsion is described well by the Saint Venant's theory and its alternative approach by Prandtl. Analytical solutions of the governing equation deduced by Saint Venant's theory have been presented for elements with circular and rectangular cross-section. Further, numerical methods based on finite element and finite difference procedures have been successfully applied to elements with practically any cross-section in order to

† Associate Professor

determine the elastic torsional rigidity.

The classical Saint Venant's approach to the torsion problem and consequently all the above mentioned analytical and numerical solutions of its governing equation, although they properly describe the elastic behaviour, fail to predict the ultimate torsional strength of concrete elements. They are based on the assumption that brittle failure occurs when the maximum developing shear stress reaches the material maximum tensile strength. By ignoring the post cracking tension softening phenomenon of the material, they consistently underestimate the ultimate torsional strength of the element. For plain concrete members the ultimate torque has been experimentally found to be roughly up to 50% greater than predicted ones (Hsu 1984). Furthermore, in the case of steel-fiber reinforced concrete elements the post cracking strength of the composite material represents an even more important part of the element strength and energy absorption capacity.

Recently, a new efficient numerical algorithm for the analysis of concrete elements in torsion has been proposed (Karayannis and Soulis 1990, Karayannis 1995a). An alternative approach properly modified and presented as a smeared crack model applicable only on plain concrete elements in torsion is also proposed (Karayannis 2000, Karayannis and Chalioris 2000). The base numerical technique can be regarded as a combination of the numerical techniques of finite element and finite difference. It uses a finite difference scheme resulting from a second-order finite element shape function for the solution of the equation of torsion and it can be applied to elements with practically any cross-section since it utilizes numerical mapping. In the present work a new stress-strain model with a non-linear post cracking branch for the material behaviour in tension, has been incorporated in this numerical approach (Karayannis 1995a) to the torsion problem. The proposed model is based on previously presented detailed models and formulae (Halpin and Tsai 1969, Lim *et al*. 1987, Gopalaratnam and Shah 1987, Bentur and Mindness 1990, Naaman *et al*. 1991) and the experimentally observed behaviour of steel-fiber concrete in direct tension. It takes into account the volume fraction of fibers, the tensile strength of concrete and parameters concerning the geometry, the orientation and the slip mechanism of the fibers. Predictions of this model for the behaviour of several steel-fiber concrete mixtures in direct tension are presented here and compared with corresponding test results conducted for this reason. From these comparisons it is shown that the model can provide a rational basis for an idealized tensile stress-strain curve that can be used in the numerical modeling of the equivalent macroscopic continuum which is implied in the analysis.

Further, by providing comparisons between analytically predicted behaviour curves and experimentally obtained ones, the validation of the proposed analysis model for the torsional response of concrete beams is presented in this paper. The experimental data used in this work comprise a series of 10 steel-fiber reinforced concrete beams tested in pure torsion for this purpose. The tested specimens include beams with rectangular, L and T cross-sections and various fiber volume fractions.

Furthermore, published experimental information was also considered collectively (22 beams) in an attempt to check the validity of the proposed approach based on test results of a broad range of parametrical studies. From these comparisons it is demonstrated that the proposed analysis describes well the behaviour of steel-fiber concrete elements in pure torsion even in the case of elements with non-rectangular cross-section.

2. Model of steel-fiber concrete in tension

Typical stress-strain responses of steel-fiber concrete specimens tested in monotonically increasing

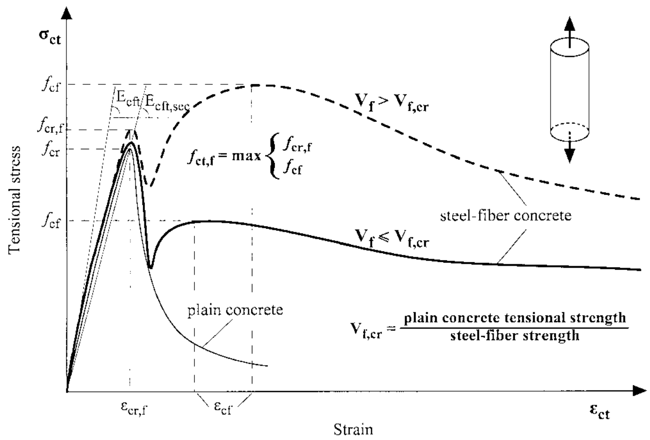

Fig. 1 Typical stress-strain response of steel-fiber concrete in direct tension

direct tension are shown in Fig. 1. Constitutive laws for plain concrete (Gopalaratnam and Shah 1985, Belarbi and Hsu 1995) and steel fiber concrete (Gopalaratnam and Shah 1987) in tension have already been proposed. In the case of steel-fiber concrete the response is generally linear until the tensile stress reaches a value a little higher than the tensile strength of the plain concrete. The fiber concrete cracks at that point and the corresponding stress and strain are termed the cracking stress $f_{cr,f}$, and strain $\varepsilon_{cr,f}$, respectively (Fig. 1). The maximum post-cracking strength f_{cf} can either be less or greater than the cracking stress. The latter requires that the amount of fibers incorporated be above a certain critical volume fraction $V_{f,cr}$ (Lim *et al.* 1987, Shah *et al.* 1978, Gopalaratnam and Shah 1987, Sorushian and Bayasi 1987) which can be expressed as

$$V_{f,\,cr} = \frac{f_{ct}}{\eta_l \eta_o \sigma_{fu}} \tag{1}$$

where f_{ct} is the tensile strength of plain concrete; η_l the ratio of the average fiber stress to the maximum fiber stress (Nathan *et al.* 1977, Lim *et al.* 1987), equal to 0.5 for $l_f \le l_{cr}$ and $\eta_l = 1 - l_f/2\,l_{cr}$ for $l_f > l_{cr}$.

Coefficient η_o is the fiber orientation factor in the elastic range (Lim *et al.* 1987) equal to $\eta_o = 0.405$; l_{cr} the length required to develop in the fiber the ultimate fiber stress σ_{fu} when a uniform ultimate bond stress τ_u is assumed at the fiber-matrix interface i.e., $l_{cr} = 0.5\sigma_{fu}\,d_f/\tau_u$. The ultimate fiber stress σ_{fu} is given as $\sigma_{fu} = 2\tau_u l_f/d_f$ for $l_f \le l_{cr}$ (slip of fiber due to failure of interfacial bond stress) and $\sigma_{fu} = f_{uf}$ for $l_f > l_{cr}$ (fiber tensile failure); where τ_u is the ultimate fiber-matrix bond stress; l_f, d_f the length and diametre of fiber, respectively and f_{uf} the fiber tensile strength.

In the present work the typical tensile response of steel-fiber concrete is approached by two types of stress-strain curves. The first type is a tri-linear curve and is used for the case that the maximum post-cracking strength f_{cf} is less than the cracking stress, i.e., for $V_f \le V_{f,cr}$ (Fig. 2a). This is justified because the observed post-cracking responses are characterized by two almost linear parts; the first one is a steep descending branch and the second one an almost horizontal straight part. For the case, though, that the maximum post-cracking strength f_{cf} is greater than the cracking stress, i.e., for $V_f > V_{f,cr}$, the adopted stress-strain relationship in order to better describe the curved post-cracking branch of the tensile response employs an exponential curve (see also Fig. 2b). In each case the criterion for the choice of the proper stress-strain curve is based on the volume fiber fraction of the

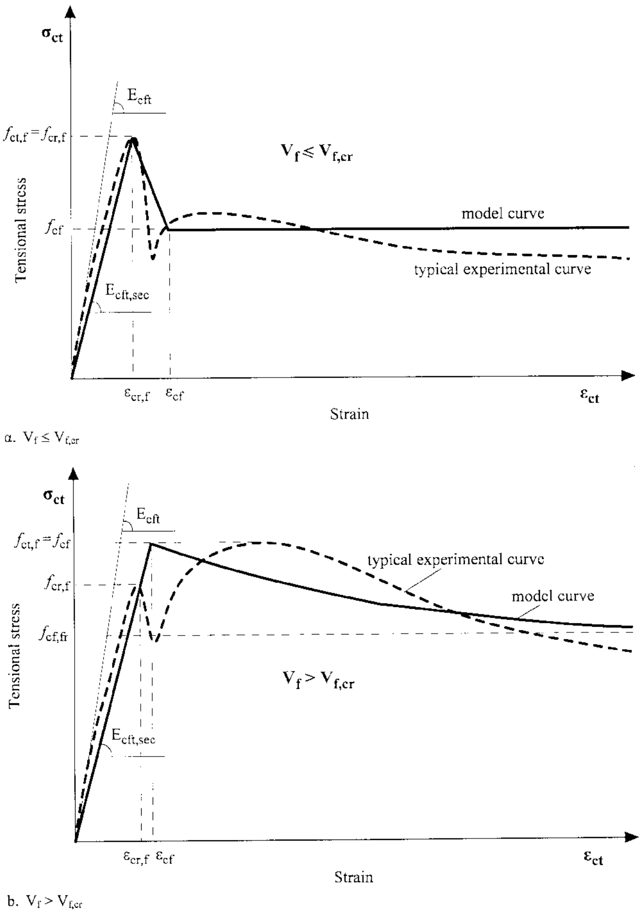

Fig. 2 Model stress-strain curves for the response of steel-fiber concrete in direct tension

concrete mixture V_f.

The elastic linear part of both model curves (Figs. 2a and b) can be determined by the cracking strain $\varepsilon_{cr,f}$, and the secant modulus of elasticity $E_{cft,sec}$ at the cracking stress, which can be given (Nathan *et al.* 1977, Lim *et al.* 1987) by the following expressions

$$\varepsilon_{cr,f} = \eta_l \eta_{oe} V_f(\varepsilon_{yf} - \varepsilon_{cr}) + \varepsilon_{cr} \tag{2}$$

where ε_{yf} is the fiber yield strain; ε_{cr} the cracking strain of plain concrete; η_{oe} the fiber orientation factor in the elastic range equal to 0.14-0.167 (Bentur and Mindness 1990); and

$$E_{cft,sec} = \frac{3}{8}E_{cfL,sec} + \frac{5}{8}E_{cfT,sec} \quad \text{(law of mixtures)} \tag{3}$$

where and $E_{cfL,sec} = E_{ct,sec}(1-V_f) + E_f V_f$ and $E_{cfT,sec} = E_f E_{ct,sec}/(E_f(1-V_f) + E_{ct,sec}V_f)$; $E_{ct,sec}$ is the secant modulus of plain concrete ($E_{ct,sec}=f_{cr}/\varepsilon_{cr}$) and E_f the fiber modulus of elasticity.

In the tri-linear curve (case $V_f \leq V_{f,cr}$) the maximum tensile strength $f_{ct,f}$ is equal to $f_{cr,f}$ and the post-cracking maximum strength f_{cf} can be calculated by the expression (Lim *et al.* 1987).

$$f_{cf} = \eta_l \eta_o \sigma_{fu} V_f \tag{4}$$

The strain value which corresponds to the post-cracking maximum strength f_{cf} (see also Fig. 2b) can be approximated (Karayannis 1995b) as

$$\varepsilon_{cf} = \alpha_f \varepsilon_{cr,f} \tag{5}$$

where $\alpha_f \approx 2$ for straight fibers and $\alpha_f = 3$ to 8 for hooked fibers ($l_f = 30$ to 50 mm) and volume fractions $V_f = 1\%$ to 3%.

In the case $V_f > V_{f,cr}$, the maximum tensile strength $f_{ct,f}$ is equal to the post-cracking maximum strength f_{cf} which is given by the Eq. (4). For the better description of the softening response of the composite material, a descending exponential curve which asymptotically tends to the horizontal line at the value $f_{cf,fr}$ (as calculated by the Eq. 7) is employed (see also Fig. 2b). This post-cracking curve is described by the equation

$$\sigma_{ct} = f_{cf,fr} + (f_{ct,f} - f_{cf,fr}) e^{-k(\varepsilon_{ct}/\varepsilon_{cf} - 1)} \tag{6}$$

where the value $f_{cf,fr}$ is given as

$$f_{cf,fr} = 2 \eta_l \eta_o \tau_{fr} V_f \, l_f / d_f \tag{7}$$

where τ_{fr} is the friction stress between fiber and matrix, and k a curve coefficient (k=0.1 to 0.7).

Further, in order to check the validity of the described model, a series of 12 plain and steel-fiber concrete specimens were tested in direct tension and the observed results are compared with the predictions of the model. The specimens are divided to three groups; the first group comprises plain concrete specimens for comparison reasons; the second one comprises specimens with straight and hooked fibers and volume fraction $V_f = 1\%$ and the third one specimens with hooked and crimped fibers and $V_f = 3\%$. The tensile specimens (Fig. 3) were tested in direct tension using a pair of specially designed grips. The extension rate was set at 0.35 mm/min while the strain was monitored by means of four LVDTs capable of reading to 0.001 mm, symmetrically fixed on a pair of hoops mounted on the test specimen. The measured characteristic response values of all tests are presented

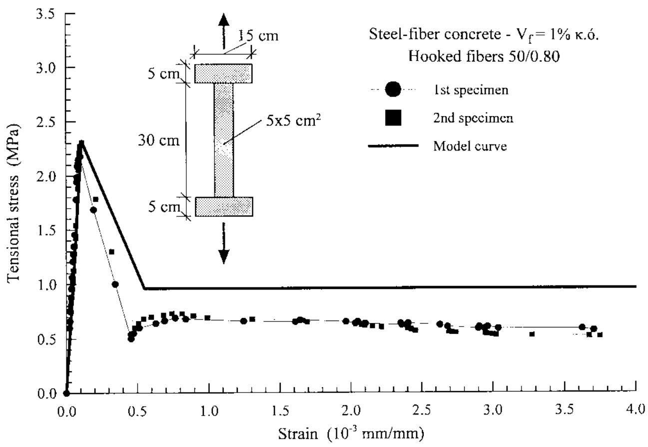

Fig. 3 Test results of two steel-fiber concrete specimens with $V_f = 1\%$ in direct tension and comparison to the model curve (case $V_f < V_{f,cr}$)

Table 1 Experimental data and comparisons to analytical results of plain and steel-fiber concrete specimens tested in direct tension

Type of fibers	Spec. No.	V_f	(a) Experimental data–(b) Predicted values–(c) Ratio exp. / pred.											
			f_{crf} (MPa)			ε_{crf} (‰ mm/mm)			$E_{cft,sec}$ (GPa)			f_{cf} (MPa)		
			(a)	(b)	(c)	(a)	(b)	(c)	(a)	(b)	(c)	(a)	(b)	(c)
No fibers	1.	–	2.17			0.098			22.14			–		
(plain concrete)	2.	–	2.05			0.110			18.64			–		
	3.	–	2.29			0.114			20.09			–		
m.v.			**2.17**			**0.107**			**20.22**					
Straight fibers	1.	1%	2.20		*0.95*	0.110		*1.00*	20.00		*0.95*	0.53		*1.12*
l_f/d_f=45/0.80	2.	1%	2.37	**2.32**	*1.02*	0.122	**0.110**	*1.10*	19.43	**21.04**	*0.92*	0.36	**0.47**	*0.76*
m.v.			**2.29**		***0.98***	**0.116**		***1.05***	19.70		***0.94***	**0.45**		***0.94***
Hooked fibers	1.	1%	2.18		*0.94*	0.100		*0.91*	21.80		*1.04*	0.70		*0.73*
l_f/d_f=50/0.80	2.	1%	2.30	**2.32**	*0.99*	0.111	**0.110**	*1.01*	20.72	**21.04**	*0.98*	0.74	**0.96**	*0.73*
m.v.			**2.24**		***0.97***	**0.106**		***0.96***	21.26		***1.01***	**0.72**		***0.75***
Hooked fibers	1.	3%	2.30		*0.87*	0.114		*0.98*	20.18		*0.89*	3.03		*1.06*
l_f/d_f=50/0.80	2.	3%	2.19	**2.65**	*0.83*	0.100	**0.117**	*0.86*	21.90	**22.70**	*0.96*	2.72	**2.87**	*0.95*
	3.	3%	2.38		*0.99*	0.110		*0.94*	21.64		*0.95*	3.10		*1.08*
m.v.			**2.29**		***0.86***	**0.108**		***0.92***	21.24		***0.94***	**2.95**		***1.03***
Crimped fibers	1.	3%	2.61		*0.99*	0.105		*0.90*	24.86		*1.09*	2.86		*1.04*
l_f/d_f=40/0.80	2.	3%	2.51	**2.65**	*0.95*	0.124	**0.117**	*1.06*	20.24	**22.70**	*0.89*	2.60	**2.76**	*0.94*
m.v.			**2.50**		***0.94***	**0.115**		***0.98***	**21.83**		***0.96***	**2.73**		***0.99***

m.v.: Mean value

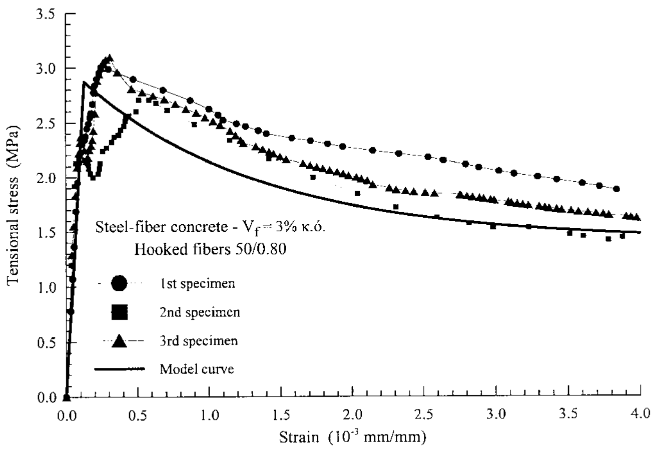

Fig. 4 Test results of three steel-fiber concrete specimens with $V_f = 3\%$ in direct tension and comparison to the model curve (case $V_f > V_{f,cr}$)

in Table 1 and compared with the corresponding predictions by the described model. Comparison between the observed behaviour of two specimens with hooked fibers and fiber fraction 1%, i.e., case $V_f \leq V_{f,cr}$, and the model predictions are presented in Fig. 3. Similar comparisons between the observed behaviour of three specimens with hooked fibers and fiber fraction 3%, i.e., case $V_f > V_{f,cr}$, and the model predictions are presented in Fig. 4. From the comparisons of these data (Table 1 and Figs. 3 and 4) it can be shown that the proposed model can be a rational basis for an idealized stress-strain curve used in the torsional analysis.

3. Analysis method

An efficient numerical algorithm for the analysis of concrete elements in torsion, recently proposed by Karayannis (1995a), properly adapted to include the previously described behavioural model for steel-fiber concrete in tension, is employed in the present work.

Considering the deformation field for the case of torsion, there prevail only two non-zero shear stress components τ_{zx}, τ_{zy} which can be expressed in terms of the stress function F as

$$\tau_{zx} = \partial F/\partial y \quad \text{and} \quad \tau_{zy} = -\partial F/\partial x \tag{8a}$$

and the resultant shear stress at a point is

$$\tau = (\tau_{zx}^2 + \tau_{zy}^2)^{1/2} \tag{8b}$$

Since only shear stresses develop on a cross-section of an element subjected to pure torsion without skew restraint, an infinitesimal element on this cross-section is in a pure shear stress state. Fig. 5 displays an infinitesimal element in pure shear stress state. From this figure it can be deduced that, in the case of pure torsion, the response can be characterized by the behaviour of the material in direct tension with tensile stress equal to the developing shear stress. This is in full compliance with conclusions deduced from early experimental efforts for the study of the behaviour of plain concrete subjected to pure torsion, which revealed that the material fails in tension rather than shear (Anderson 1935, Cowan 1965).

If G denotes the shear modulus of elasticity which may depend on x and y and ϑ is the angle of twist per unit length, the governing equation is given by

$$\frac{\partial}{\partial x}\left(\frac{1}{G}\frac{\partial F}{\partial x}\right) + \frac{\partial}{\partial y}\left(\frac{1}{G}\frac{\partial F}{\partial y}\right) = -2\vartheta \tag{9}$$

The domain of interest is discretized by 8-node isoparametric elements. That is, all physical elements (x, y) regardless of their configuration are mapped to the (ξ, η) coordinates (isoparametric mapping) such that $-1 \le \xi \le 1$ and $-1 \le \eta \le 1$, where the nodes of the mapped elements are located at $\xi = \pm 1$ and $\eta = \pm 1$. If (x_i, y_i) are the Cartesian coordinates of the nodes of an element then the coordinates of any point in an element can be obtained as

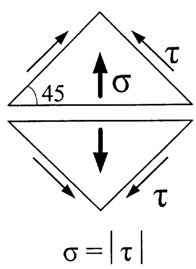

Fig. 5 A finite element in pure shear and equivalent tension state

$$x = \sum_{i=1}^{8} (N_i x_i), \quad y = \sum_{i=1}^{8} (N_i y_i) \tag{10}$$

where N_i are the shape functions associated with the element nodes (Karayannis 1995a).

Let J be the transformation matrix and ^{T} denotes the transpose matrix; then

$$H = J^T J = \begin{bmatrix} h_{11} & h_{12} \\ h_{21} & h_{22} \end{bmatrix} \tag{11}$$

It follows that if H^{-1} is the inverse of matrix H, the shear stress components in the computational field are derived as

$$\begin{bmatrix} \tau_{z\eta} \\ \tau_{z\xi} \end{bmatrix} = H^{-1} \begin{bmatrix} \partial F/\partial \xi \\ \partial F/\partial \eta \end{bmatrix} \quad \text{such that} \quad \begin{bmatrix} -\tau_{zy} \\ \tau_{zx} \end{bmatrix} = J \begin{bmatrix} \tau_{z\eta} \\ \tau_{z\xi} \end{bmatrix} \tag{12}$$

If Δ denotes the determinant of matrix J and G is the shear modulus of elasticity then the governing equation of torsion (Eq. 9) can be transformed into the local (ξ, η) domain as

$$\frac{\partial}{\partial \xi}\left(\frac{\Delta}{G}\tau_{z\eta}\right) + \frac{\partial}{\partial \eta}\left(\frac{\Delta}{G}\tau_{z\xi}\right) = -2\vartheta\Delta \tag{13}$$

The derivatives of the quantities x, y, F, $(\Delta\tau_{z\eta}/G)$ and $(\Delta\tau_{z\xi}/G)$ at the center i, j of an element are calculated. Using these derivatives the equation of torsion in the local coordinate system or computational grid (Eq. 13) may be discretized as

$$\left(\frac{\Delta}{G}\tau_{z\eta}\right)_{i,j+1} - \left(\frac{\Delta}{G}\tau_{z\eta}\right)_{i,j-1} + \left(\frac{\Delta}{G}\tau_{z\xi}\right)_{i+1,j} - \left(\frac{\Delta}{G}\tau_{z\xi}\right)_{i-1,j} = -2\vartheta\Delta_{i,j} \tag{14}$$

Using Eq. (12), the shear stress components in the local system are derived as

$$(\tau_{z\eta})_{i,j} = (h'_{11})_{i,j}\frac{F_{i,j+1} - F_{i,j-1}}{2} + (h'_{12})_{i,j}\frac{F_{i+1,j} - F_{i-1,j}}{2} \tag{15a}$$

$$(\tau_{z\xi})_{i,j} = (h'_{21})_{i,j}\frac{F_{i,j+1} - F_{i,j-1}}{2} + (h'_{22})_{i,j}\frac{F_{i+1,j} - F_{i-1,j}}{2} \tag{15b}$$

Hence, the governing equation (Eq. 14) in a finite differences form can be approximated as

$$\begin{aligned} &\alpha_1 F_{i-1,j-1} + \alpha_2 F_{i-1,j+1} + \alpha_3 F_{i+1,j+1} + \alpha_4 F_{i+1,j-1} + \alpha_5 F_{i-2,j} \\ &+ \alpha_6 F_{i,j+2} + \alpha_7 F_{i+2,j} + \alpha_8 F_{i,j-2} + \alpha_9 F_{i,j} = -8\vartheta\Delta_{i,j} \end{aligned} \tag{16}$$

where α_1, α_2,... α_9 are expressions of the quantities G, Δ and the elements h'_{11}, h'_{12}, h'_{22} of the matrix H^{-1}, at the appropriate nodes (Karayannis 1995a). Afterwards, an internal iterative procedure is performed which yields the solution of the transformed equation of torsion (Eq. 13).

4. Experimental program and verification

4.1. Experimental program - specimen characteristics

A series of 10 steel-fiber concrete beams were constructed and tested in pure torsion. Two of them, RP1 and RP3, were rectangular beams with cross-section dimensions 10/20 cm and fiber volume fraction $V_f = 1\%$ and 3%, respectively. Two specimens, LsP1 and LP1, were beams with $V_f = 1\%$ and L-cross-section with flange width equal to 15 and 20 cm, respectively. The rest of the 6 specimens were beams with $V_f = 1\%$ and 3%, and a T-cross-section with various types and widths of flange. Geometrical details and cross-sections for all specimens are presented in Fig. 6 and Table 2. The cement used in this experimental work was a locally manufactured general purpose ordinary Portland type cement (type 35IIa, Greek type pozzolan cement containing 10% fly ash) whereas the steel fibers were hooked fibers with l_f/d_f= 30/0.80 mm. Sand with a high fineness modulus and coarse aggregates with a maximum size of 9.5 mm (3/8 in.) were used. The concrete mixture was made using cement, sand and crushed aggregates in a proportion 1:2.8:1.2, respectively, and water to cement ratio equal to 0.43. Supplementary compression and splitting tests in order to determine the compression strength of the particular concrete and the tensile strength of the composite mixture were also included in the program and results are given in Table 2. The total length of the beams,

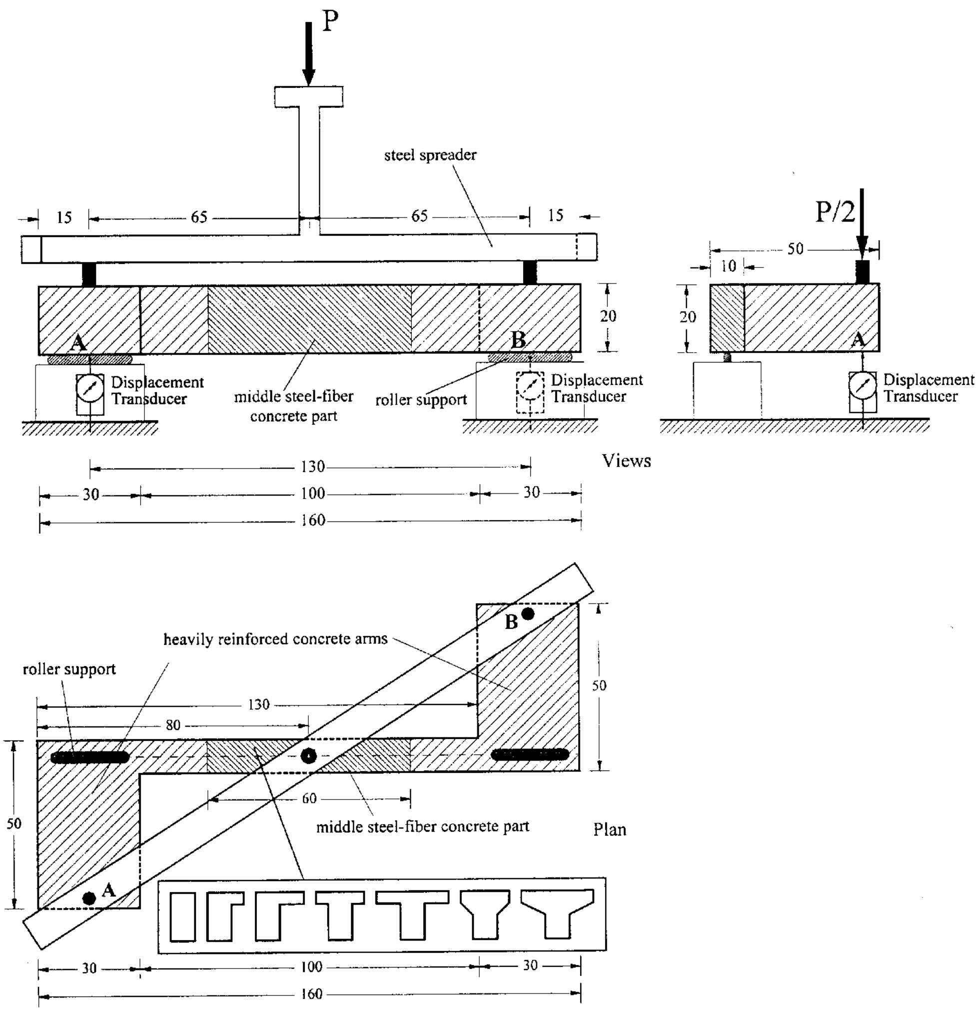

Fig. 6 Torsion test setup and geometrical details of beams tested in torsion

Table 2 Cross-sections, experimental data and comparisons to analytical predictions of steel-fiber reinforced concrete beams tested in pure torsion

Code name	Cross-section	V_f	Experimental data				Analytical predictions	
			f'_c (MPa)	$f_{ct,split}$ (MPa)	T_{exp} (kNcm)	K_{exp} (†)	T_{pred} (T_{exp}/T_{pred}) (kNcm)	K_{pred} (K_{exp}/K_{pred}) (†)
RP1	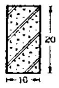	1%	19.80	2.05	184.22	3235	165.20 (1.12)	3018 (1.07)
RP3	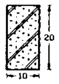	3%	19.26	2.26	195.00	3405	194.61 (1.00)	3235 (1.05)
LsP1	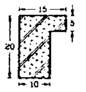	1%	21.00	2.25	221.27	4539	229.66 (0.96)	5792 (0.78)
LP1	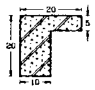	1%	30.00	2.85	265.25	6103	278.78 (0.95)	7605 (0.80)
TsP1	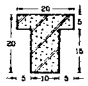	1%	25.00	2.36	272.33	6450	294.37 (0.93)	8072 (0.80)
TP1	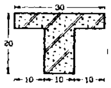	1%	29.14	2.83	296.23	8907	335.37 (0.88)	11440 (0.78)
THsP1	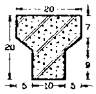	1%	27.26	2.03	338.66	8947	320.99 (1.06)	9328 (0.96)
THsP3	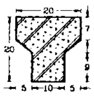	3%	33.04	3.24	369.44	8697	377.94 (0.98)	11110 (0.78)
THP1	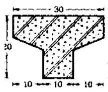	1%	26.00	1.91	405.00	15705	411.27 (0.98)	14187 (1.11)
THP3	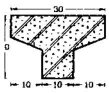	3%	29.51	4.36	442.00	15365	453.39 (0.97)	16429 (0.94)

† $\left(10^3 \frac{\text{kN cm}^2}{\text{rad}}\right)$

common for all specimens, is equal to 1.60 m and is divided in three parts; two heavily reinforced end parts and one steel-fiber reinforced middle part. The end parts were properly reinforced so that they can without cracking bear the loading which is imposed at the ends of the beams. The middle steel-fiber concrete part was 60 cm long and was the part where the cracking and, finally, the failure was localized during the test (Fig. 6). The experimental setup is shown in Fig. 6. All specimens were tested under the action of pure torsion. They were supported on two roller supports 1.30 m apart. These supports ensured that the test beams were free to twist and to elongate longitudinally at both ends. The load was applied on the properly configured ends of each tested beam, through a steel spreader as shown in Fig. 6. Displacement transducers placed at both end concrete arms (at the points of loading A and B in Fig. 6) measured the deflections of the arms as the beam twisted. The accuracy of the used DTs was 0.01 mm. The average angle of twist was calculated from these deflections.

4.2. Test results-comparisons with analytical predictions

All specimens were tested using monotonically increasing torque moment. The initial elastic torsional stiffness K_{exp} ($=T/\theta$) and the ultimate torque moment T_{exp}, as measured from the tests, for all tested specimens are presented in Table 2. Also included in Table 2 are the plain concrete compressive strength and the steel-fiber concrete tensile strength as deduced from complimentary compressive and split tests, respectively; all strength values are given as the mean value of three cylinders for each case and specimen.

Analyses for the prediction of the torsional behaviour of each tested beam using the proposed approach were performed and the predicted values for the initial torsional stiffnesses K_{pred} and the ultimate torque moments T_{pred}, for all specimens, were calculated. The predicted values for the initial torsional stiffness K_{pred} and the ultimate torque moment T_{pred} of all specimens are also presented in Table 2 and compared with the measured ones. From this table it can be observed that the ratio $T_{\mathrm{exp}}/T_{\mathrm{pred}}$ for the total of the examined cases (10 beams) has mean value $(T_{\mathrm{exp}}/T_{\mathrm{pred}})_{\mathrm{mean}} =$ 0.983 with standard deviation 0.065 and ranges from 1.00 to 1.12 for the rectangular beams and from 0.88 to 1.06 for the non-rectangular ones. Also, the ratio $K_{\mathrm{exp}}/K_{\mathrm{pred}}$ for the total of the examined cases (12 beams) has mean value $(K_{\mathrm{exp}}/K_{\mathrm{pred}})_{\mathrm{mean}} =$ 0.907 with standard deviation 0.134 and ranges from 1.05 to 1.07 for the rectangular beams and from 0.78 to 1.11 for the non-rectangular ones. The predicted torsional behaviour curves for the RP3 rectangular beam, the LP1

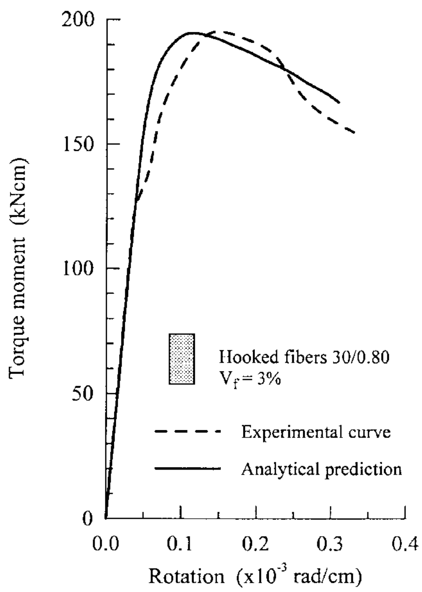

Fig. 7 Experimental curve and comparison to the predicted one for a rectangular beam with hooked fibers and volume fraction V_f=3%

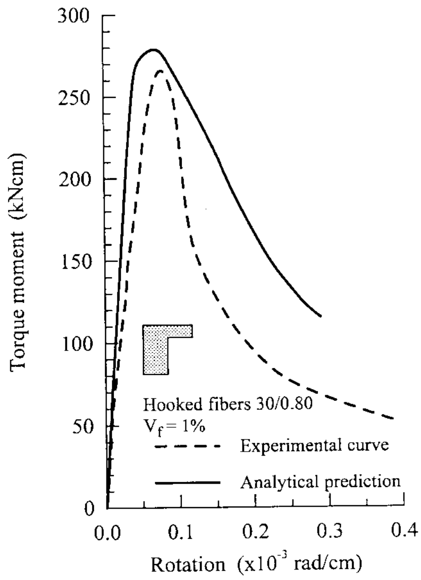

Fig. 8 Experimental curve and comparison to the predicted one for a beam with L-cross-section and hooked fibers volume fraction $V_f = 1\%$

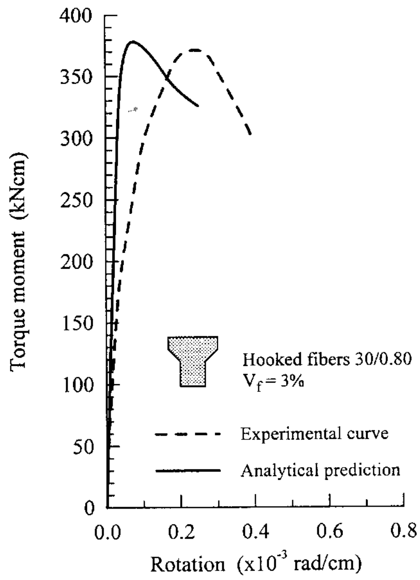

Fig. 9 Experimental curve and comparison to the predicted one for a T-beam with small flange (b/b_o=2.0) and hooked fibers volume fraction $V_f = 3\%$

beam with L-cross-section are presented and compared with the experimental ones in Figs. 7 and 8, respectively. Furthermore, the predicted torsional behaviour curves for the T-beams THsP3, THP1 and THP3 are also presented and compared with the experimental ones in Figs. 9, 10a and 10b, respectively.

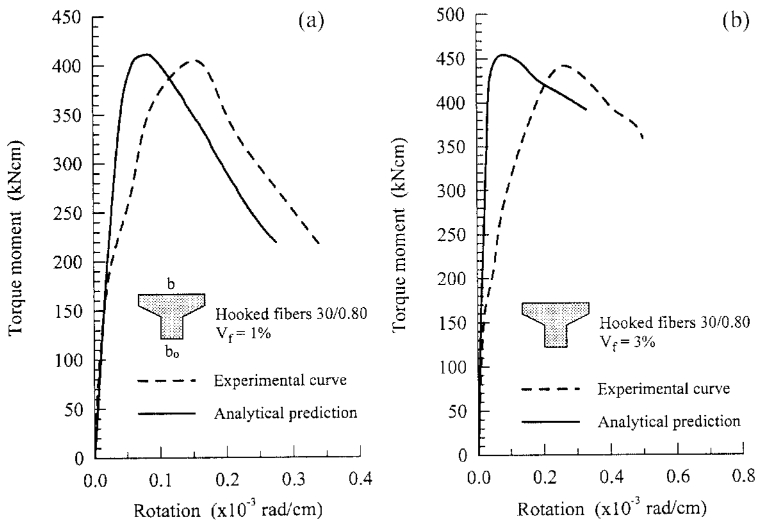

Fig. 10 Experimental curves and comparisons to the predicted ones for two T-beams with flange ratio b/b_o=3.0 and hooked fibers volume fractions V_f = 1% and 3%

5. Comparisons with results of other experimental studies

The experimental information compiled from published parametric studies, for the validation of the present approach contains a total of 22 beams (Mansur 1982, Mansur and Paramasivam 1985, Craig *et al.* 1986, Wafa *et al.* 1992). Most of the tests included were done over the last twenty years in U.S. and other countries. Tests compiled were steel fiber-reinforced concrete beams with various types of steel fibers and fiber fractions (see also Table 3) subjected to pure torsion. In all cases the cross-sections were rectangular ones and the depth to width aspect ratio of the examined beams is varied from 1.0 to 2.5.

Analyses for the prediction of the torsional behaviour of each tested beam using the proposed approach were performed and the predicted values for the ultimate torque moments T_{pred}, for all specimens, were calculated. Test information and proposed model data for all specimens are presented in Table 3. In the same table the predicted values for the ultimate torque moment T_{pred} are also presented and compared with the measured ones T_{exp}. From the results it can be seen that the mean value of the ratio $T_{\text{exp}}/T_{\text{pred}}$ is $(T_{\text{exp}}/T_{\text{pred}})_{\text{mean}}$=1.013 with standard deviation 0.063. Experimental curves and comparison to the predicted ones for 4 rectangular steel-fiber reinforced concrete beams in pure torsion compiled from Wafa *et al.* (1992) are shown in Fig. 11. Further, experimental curves and comparisons to the predicted ones for 6 rectangular steel fiber-reinforced concrete beams in pure torsion compiled from Craig *et al.* (1986) are presented in Fig. 12. In the first case the type of steel-fibers was hooked fibers with l_f/d_f=60/0.80 mm and the volume fraction varied from 0.5% to 2.0%. In the second case (Fig. 12) two types of hooked steel-fibers were used (l_f/d_f= 30/0.50 mm and 50/0.50 mm) and the volume fractions varied from 0.7% to 2.0%. The predicted values for the ultimate torque generally are in a very good agreement with the measured ones (see also Table 3). The discrepancies between the computed and the measured response curves, which can be observed in the torque-rotation plots, for some of the specimens presented in Fig. 12 can be attributed to the fact that two kinds of steel-fibers (l_f/d_f= 30/0.50 mm and 50/0.50 mm) were simultaneously used in the same mixture (Craig *et al.* 1980). In the case of beam B1.0-0 of Fig. 11

Table 3 Steel fiber-reinforced concrete beams from literature, tested in pure torsion; measured data and comparisons with analytical predictions

Code name	b/h (cm/cm)	l_f/d_f (mm/mm)	V_f† (%)	f'_c (MPa)	f_r (MPa)	$f_{ct,f}$‡ (MPa)	T_{exp} (kNcm)	T_{pred} (kNcm)	$\frac{T_{exp}}{T_{pred}}$
Wafa *et al.* (1992)									
B0.5-0		60/0.80	0.5	35.10	4.94	3.21	299.0	294.5	1.02
B1.0-0	10/25	60/0.80	1.0	39.08	6.94	3.29	280.0	302.0	0.93
B1.5-0		60/0.80	1.5	41.42	7.23	3.36	356.0	315.6	1.13
B2.0-0		60/0.80	2.0	40.99	9.06	3.43	332.0	322.5	1.03
Craig *et al.* (1986)									
P2		30/0.50	0.7	40.00	–	3.63	945.6	915.8	1.03
P3		50/0.50	1.0	43.45	–	3.70	877.8	954.3	0.92
P4	15/30	30/0.50	1.5	35.86	–	3.83	860.8	958.8	0.90
P6		50/0.50	2.0	47.59	–	3.96	1174.9	1089.4	1.08
P7		30/0.50 +50/0.50	0.75 +0.75	40.00	–	3.96	1045.0	1009.9	1.03
P8		30/0.50 +50/0.50	1.0 +1.0	45.52	–	3.83	1113.9	1069.3	1.04
Mansur (1982)									
							96.1		1.03
A	10/10	30/0.40	0.75	34.20	4.43	3.10	99.0	93.4	1.06
(3 specimens)				cube 15cm			101.0		1.08
							166.8		1.04
B	10/15	30/0.40	0.75	34.20	4.43	3.10	164.8	160.2	1.03
(3 specimens)				cube 15cm			162.4		1.01
							210.9		0.94
C	10/20	30/0.40	0.75	34.20	4.43	3.10	205.0	224.6	0.91
(3 specimens)				cube 15cm			208.9		0.93
Mansur & Paramasivam (1985)									
							152.0		1.05
T-1	10/15	30/0.40	0.75	–	3.90	2.75	149.6	144.7	1.03
(3 specimens)							153.6		1.06
								Mean value:	**1.013**
								Standard deviation:	**0.063**

†Hooked fibers
‡Values calculated based on the proposed model

(Wafa *et al.* 1990) the observed discrepancy is mainly attributed to experimental deficiencies in instrumentation.

6. Conclusions

The behavioral model for the tensile response of steel-fiber concrete and the analysis proposed in

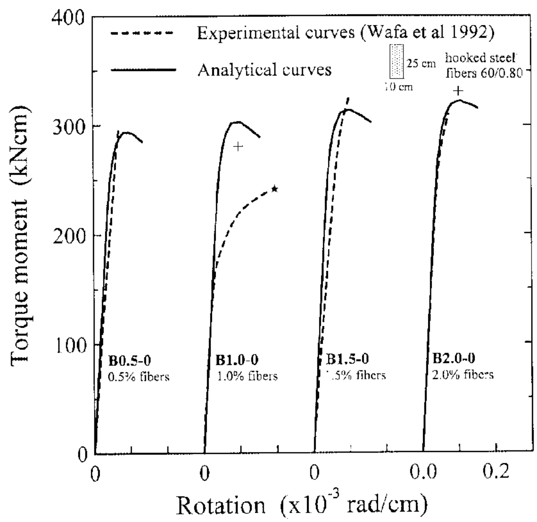

Fig. 11 Experimental curves and comparisons to the predicted ones for 4 rectangular steel fiber-reinforced concrete beams in pure torsion compiled from Wafa *et al.* (1992)

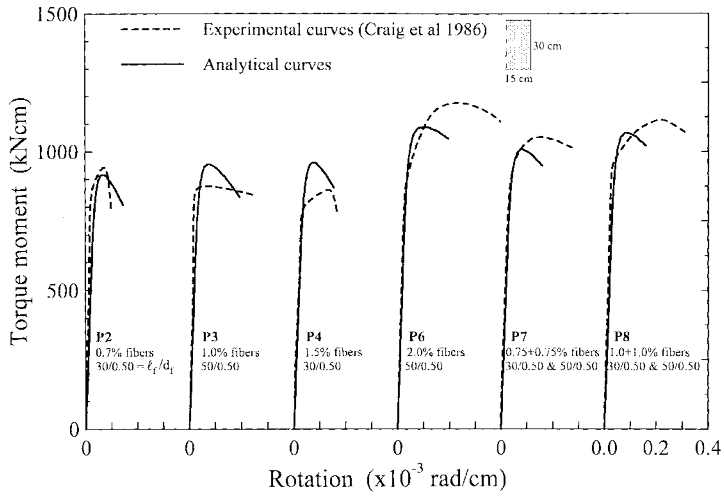

Fig. 12 Experimental curves and comparisons to the predicted ones for 6 rectangular steel fiber-reinforced concrete beams in pure torsion compiled from Craig *et al.* (1986)

this work allow for a realistic modeling of the entire response process of a steel-fiber reinforced concrete element in torsion. This has been demonstrated by means of comparisons between predicted and experimental behaviour curves. The experimental program reported in this study comprises 12 plain and steel fiber specimens tested in direct tension and a series of 10 beams, 1.60 m long, with various cross-sections and steel-fiber fractions tested in pure torsion. Furthermore, experimental data for 22 steel fiber-reinforced beams compiled from published works are also used in an attempt to establish the validity of the described approach based on test results of a broad range of studies. The conclusions drawn from the presented comparisons, imply that the applied model can successfully describe the behaviour of a steel-fiber concrete element in torsion and the developed analysis yields realistic torsion versus rotation curves for the entire response of elements with rectangular, L- and T-cross-sections subjected to monotonically increased torsion.

Acknowledgements

The contribution of Dr. C. Chalioris on the computational work is greatly appreciated.

References

Anderson, P. (1935), “Experiments with concrete in torsion”, *Trans. ASCE*, **100**, 949-983.

ACI Committee 544 (1982), State-of-the-Art Report on Fibre Reinforced Concrete, Report No. 44.IR-82 (Reapproved 1986), American Concrete Institute, Detroit.

Belarbi, A. and Hsu, T.T.C. (1995), “Constitutive laws of softened concrete in biaxial tension-compression”, *ACI Structural Journal*, **92**(5), 562-573.

Bentur, A. and Mindness, S. (1990), *Fibre Reinforced Cementitious Composites*, Elsevier Applied Science, New York.

Cowan, H.J. (1965), *Reinforced and Prestressed Concrete in Torsion.* Edward Arnold (Publishers) Ltd., London.

Craig, R.J., Parr, J.A., Germain, E., Mosquera, V. and Kamilares, S. (1986), “Fiber reinforced beams in torsion”, *J. ACI*, **83**(6), 934-942.

Gopalaratnam, V.S. and Shah, S.P. (1985), “Softening response of plain concrete in direct tension”, *J. of A.C.I.*, **82**(27), 310-323.

Gopalaratnam, V.S. and Shah, S.P. (1987), “Tensile failure of steel fiber-reinforced mortar”, *J. of Engineering Mechanics, ASCE*, **113**, 635-652.

Halpin J.C. and Tsai S.W. (1969), *Effects of Environmental Factors on Composite Materials*, AFML-TR 67-423.

Hsu, T.T.C. (1984), *Torsion of Reinforced Concrete.* Van Nostrand Reinhold, New York.

Karayannis, C.G. and Soulis, J.V. (1990), “A numerical method for torsional analysis of structural elements”, *J. Computers & Structures*, **36**(4), 755-768.

Karayannis, C.G. (1995a), “Torsional analysis of flanged concrete elements with tension softening”, *J. Computers & Structures*, **54**(1), 97-110.

Karayannis, C.G. (1995b), “A numerical approach to steel-fibre reinforced concrete under torsion”, *J. Structural Engineering Review*, **7**(2), 83-91.

Karayannis, C.G. (2000), “A Smeared Crack Analysis for Concrete in Torsion” *Structural J. ASCE*, to appear.

Karayannis, C.G. and Chalioris, C. (2000), “Experimental validation of a smeared analysis for concrete in torsion”, *Structural J. ASCE*, to appear.

Lim, T.Y., Paramasivam, P. and Lee, S.L. (1987), “Analytical Model for Tensile Behavior of Steel-Fiber Concrete”, *ACI Materials Journal*, **84** (4), 286-298.

Mansur, M.A. (1982), “Bending-torsion interaction for concrete beams reinforced with steel fibres”, *Magazine of Concrete Research*, **34**(121), 182-190.

Mansur, M.A. and Paramasivam, P. (1985), “Fiber reinforced concrete beams in torsion, bending, and shear”, *ACI J.*, **82**(2), 33-39.

Nathan, G.K., Paramasivam, P. and Lee, S.L. (1987), “Tensile behavior of fiber reinforced cement paste”, *J. Ferrocement*, **8** (2), 59-79.

Wafa, F.F., Hasnat, A. and Tarabolsi, O.F. (1992), “Prestressed fiber reinforced concrete beams subjected to torsion”, *J. ACI*, **89**(3), 272-283.